Atmospheric Environment 246 (2021) 118080

Contents lists available at ScienceDirect

Atmospheric Environment

journal homepage: http://www.elsevier.com/locate/atmosenv

The effect of recent controls on emissions and aerosol pollution at city scale: A case study for Nanjing, China

Yu Zhao [a,b,*], Yiwei Huang [a,c], Fangjian Xie [d], Xin Huang [e], Yang Yang [a]

[a] State Key Laboratory of Pollution Control, Resource Reuse and School of the Environment, Nanjing University, 163 Xianlin Rd., Nanjing, Jiangsu, 210023, China
[b] Jiangsu Collaborative Innovation Center of Atmospheric Environment and Equipment Technology (CICAEET), Nanjing University of Information Science & Technology, Jiangsu, 210044, China
[c] Shanghai Academy of Environmental Sciences, 508 Qinzhou Rd., Shanghai, 200233, China
[d] Nanjing Academy of Environmental Protection Science, 175 Huju Rd., Nanjing, Jiangsu, 210013, China
[e] School of Atmospheric Science, Nanjing University, 163 Xianlin Ave., Nanjing, Jiangsu, 210023, China

HIGHLIGHTS

- The emissions of most species were largely reduced in Nanjing from 2012 to 2016.
- The city-scale emission inventory was evaluated based on observation and simulation.
- Emission control played an important role on $PM_{2.5}$ concentration reduction.
- Industry was the main contributor to the reduced emissions and $PM_{2.5}$ levels.
- Meteorology was more influential on the $PM_{2.5}$ variation for individual months.

ARTICLE INFO

Keywords:
Emission reduction
Aerosol pollution
Meteorology
City

ABSTRACT

We selected a typical developed city in east China, Nanjing, to evaluate the effect of recent national and local policies of air pollution control on emissions and air quality at city scale. Using a bottom-up methodology, the annual emissions of SO_2, NO_X, CO, NH_3, primary fine particle matters ($PM_{2.5}$), black carbon, and organic carbon were estimated to decline 70%, 22%, 49%, 72%, 64%, 65%, and 86%, respectively, while a slight increase was found for the non-methane volatile organic compounds (VOCs) during 2012–2016. The inter-annual change in NO_X emissions was consistent with that in tropospheric NO_2 column from satellite observation. Using air quality modeling (AQM), the city-scale emission inventory was further evaluated through comparisons between the simulated and observed concentrations of selected species. For SO_2, NO_2 and $PM_{2.5}$, the normalized mean bias (NMB) and normalized mean errors (NMEs) for most cases were within 20% and 50% respectively, implying the reliability of the emission inventory. Regarding chemistry species, the modeling performance was better for sulfate and black carbon than nitrate and ammonium. From 2012 to 2016, the average of monthly $PM_{2.5}$ concentrations for January, April, July, and October in Nanjing was found to decline 28% and 25% with AQM and ground observation, respectively, implying the benefit of emission control on aerosol pollution. Extra simulations with fixed emissions or meteorology conditions for 2012 and 2016 were conducted to understand the effects of emission control and meteorology variation on the reduced aerosol pollution.

1. Introduction

High concentration of $PM_{2.5}$ (particles with aerodynamic diameter smaller than 2.5 μm) is a severe issue for China. This increased air pollution can be attributed to the fast development of industry and growth of energy consumption, particularly in areas with large populations and intensive industry including the Beijing-Tianjin-Hebei (BTH) (Chen et al., 2014; He et al., 2012; Tao et al., 2017) and the Yangtze River Delta (YRD) region (Ming et al., 2017; Wang et al., 2016). To tackle the heavy aerosol pollution, China issued the new National

* Corresponding author State Key Laboratory of Pollution Control, Resource Reuse and School of the Environment, Nanjing University, 163 Xianlin Rd., Nanjing, Jiangsu, 210023, China.
E-mail address: yuzhao@nju.edu.cn (Y. Zhao).

https://doi.org/10.1016/j.atmosenv.2020.118080
Received 18 February 2020; Received in revised form 7 November 2020; Accepted 11 November 2020
Available online 14 November 2020
1352-2310/© 2020 Elsevier Ltd. All rights reserved.

Ambient Air Quality Standard (NAAQS) of 35 μg/m^3 for $PM_{2.5}$ in 2012 (MEP, 2012), and has been implementing the Air Pollution Prevention and Control Action Plan (APPCAP) across the country since 2013 (Zhang et al., 2019). On top of the national policy, provinces and cities were encouraged to conduct more stringent measures based on their local emissions and pollution conditions to improve the air quality.

The efforts of national pollution control proved successful. According to the Multi-resolution Emission Inventory for China (MEIC, http://www.meicmodel.org/), the emissions of SO_2, NO_X, and primary $PM_{2.5}$ were reduced 62%, 17%, and 35%, respectively from 2010 to 2017 (Zheng et al., 2018). Accordingly, reduced tropospheric vertical column densities (VCD) of SO_2 and NO_2 were detected through satellite observation (Ding et al., 2017; Liu et al., 2016; Li et al., 2017; Xia et al., 2016), and the annual average concentrations of $PM_{2.5}$ were monitored to decline 40% from 2013 to 2017 for cities involved in the national monitoring network. In particular, BTH and YRD had their $PM_{2.5}$ concentrations reduced 40% and 34% for the period, respectively (MEE, 2018). Compared to the national and regional scales, however, the benefits of recent controls on emissions and air quality at city level were less quantified, attributed largely to the heterogeneity of emission sources and pollution control measures. Cities are the basic administrative modules of air quality management and implementation of pollution control measures. Tracking the variations in emission sources and exploring the corresponding response of air quality with chemistry transport modeling could be of great importance for understanding the driving forces of air quality change. Given the increased challenge in air quality simulation at finer spatial resolution (Zheng et al., 2017), more careful investigations are needed for the individual emission sources with complicated manufacturing technologies and various air pollutant control devices (APCDs).

Besides quantification of emissions, increased attention has been paid to the roles of emissions and meteorology on the changed air quality, which could improve the understanding of the benefits of emission abatement, and help policy making of air pollution control. A series of studies have been conducted to estimate the impacts of emissions and meteorological conditions on inter-annual variation in ambient aerosols, ozone (O_3) or outflow of aerosols in China (Lou et al., 2015; Mao et al., 2016; Mu and Liao, 2014; Yang et al., 2014). By fixing the emission data or meteorological conditions in air quality models, they found that the changes in emissions dominated the long-term (e.g., decade) change in air quality but meteorology played a more important role on the inter-annual variation.

In general, current studies, both on the inter-annual emission variation and its impact on air quality, focused on relatively large spatial scales, e.g., continental or national scale. The city-level emission data for multiple years since recent APPCPA were still lacking, and the role of emission change on reduced concentration was insufficiently evaluated at city scale. The knowledge remained incomplete on the effectiveness of emission controls on the air quality. Here, we select Nanjing, a typical industrial city in the YRD, to evaluate the effects of recent controls on emissions and aerosol pollution (see Fig. 1 for the city location). Nanjing consumed extremely large amount of coals and suffered the most haze days (226 out of 365) among all of China's provincial capital cities in 2012 (Zhao et al., 2015), and it has been conducting various measures to control air pollutant emissions since then. Clear progress has been achieved, with the annual average concentrations of $PM_{2.5}$ reduced from 77 in 2013 to 48 μg/m^3 in 2016 (NJBEE, 2017). In this work, we first quantified the inter-annual changes in air pollutant emissions for Nanjing with a bottom-up methodology and then evaluated the city-scale emission inventory based on available satellite/ground observation and air quality modeling. The contribution of emission reduction to the reduced $PM_{2.5}$ concentrations was further analyzed to

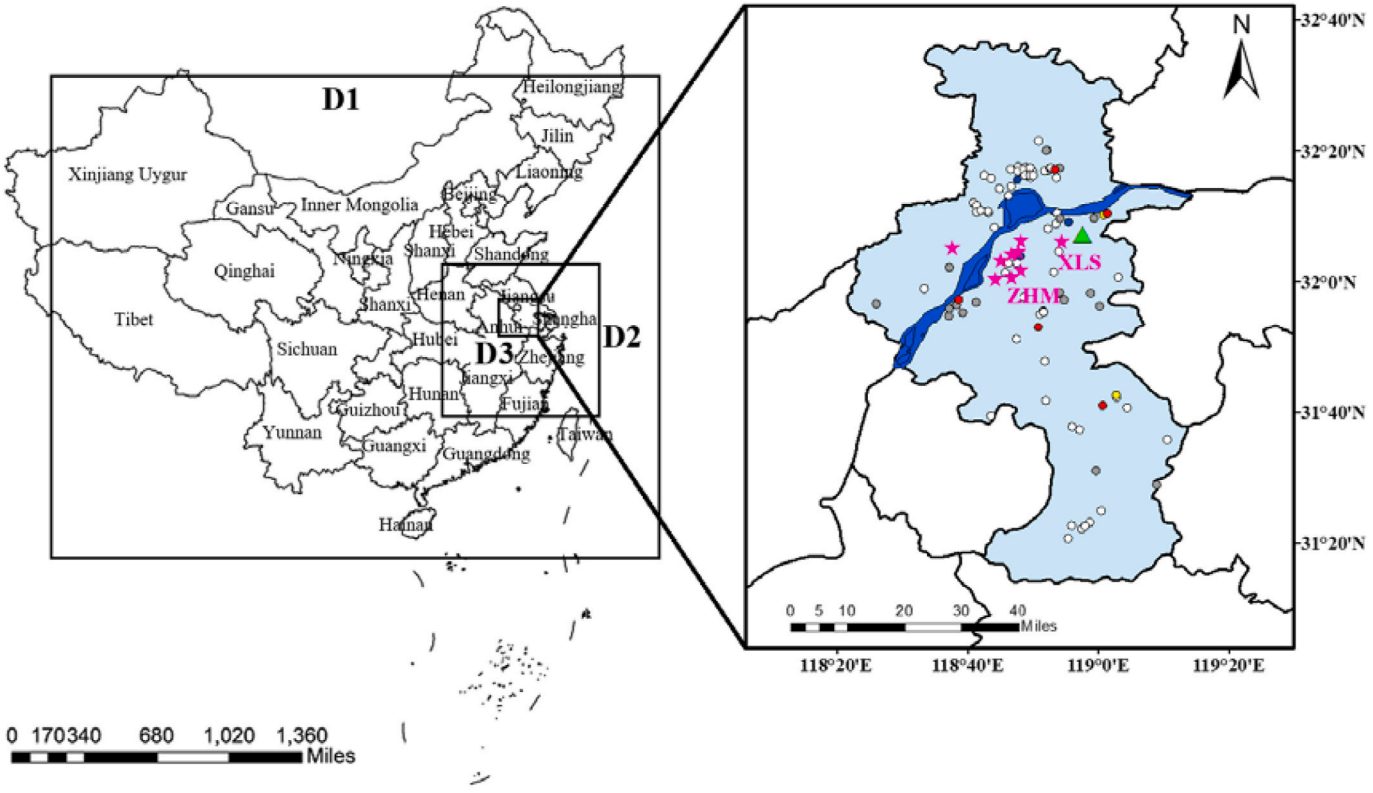

Fig. 1. The three nested modeling domains with the geographic locations of Nanjing (the blue area) and the nine state-operated air quality monitoring sites (pink stars) and SORPES (green triangle) in the city. In particular, two of the state-operated sites, XLS and ZHM, are labeled. The locations of major polluting sources are marked by colored dots including power plants (red), iron & steel plant (yellow), cement factory (grey), oil exploitation/refiner plants (blue), and chemical industry plants (white). The thick blue line indicates the Yangtze River. (For interpretation of the references to color in this figure legend, the reader is referred to the Web version of this article.)

reveal the benefits of pollution control efforts on air quality for the city.

2. Data and method

2.1. Development of emission inventories for 2012–2016

The annual emissions in Nanjing from 2012 to 2016 were estimated for SO_2, NO_2, CO, NH_3, non-methane volatile organic compounds (VOCs), primary $PM_{2.5}$, elemental carbon (EC), and organic carbon (OC). Six main source categories were included in the emission inventory, i.e., power sector, industry, transportation (including on-road and non-road subcategories), the residential & commercial sector (including fossil fuel, biofuel, and biomass open burning subcategories), solvent use (for VOCs only), and agriculture (including livestock farming and fertilizer use for NH_3 only).

To improve the emission estimation at city and provincial levels in the YRD region, our previous studies developed a methodology that incorporated the best available local information of individual power and industrial plants and the traffic flows of main road nets (Zhao et al., 2015, 2017a; Zhou et al., 2017). Briefly, the annual emissions were calculated with Eq. (1):

$$E_i = \sum_{j,m} AL_{i,j,m} \times EF_{i,j,m} \times \left(1 - \eta_{i,j,m}\right) \quad (1)$$

where i, j and m represented the pollutant species, individual plant (for point sources)/source type (for area and mobile sources), and fuel/technology type, respectively; AL was the activity level data; EF was the uncontrolled emission factor (the emissions per unit of activity level); and η was the removal efficiency of specific APCD.

In this work, we followed the methodology mentioned above to collect the activity data by source category in Nanjing, and the emission factor databases established in those studies (Zhao et al., 2015, 2017a; Zhou et al., 2017) were directly applied. The information of individual emission sources including the activity data and the removal efficiencies of APCDs was compiled for each year during the research period. The changes in emission factors between 2012 and 2016 were attributed mainly to the improved controls. For example, the penetrations and removal efficiencies of APCDs in power and industrial sectors were collected for individual plants based on the official environmental statistics, Pollution Source Census (PSC, internal data), and on-site investigations. The annual averages by source type were summarized in Table S1 in the supplement. Clear growth can be found for both the penetrations and removal efficiencies of APCDs, along with the improved use and management of APCDs from 2012 to 2016. Fig. S1 in the supplement illustrates the populations of on-road vehicles with different emission control stages for 2012 and 2016. With more and more stringent emission standards gradually implemented, the fractions of Stage V (the 5th phase of China's national emission standard for vehicles, equal to Euro V) passenger cars and heavy duty vehicles increased from 0% to 20% and from 0 to 16%, respectively, during 2012–2016, leading to the clearly reduced emission factors as summarized in Table S2 in the supplement. Furthermore, shutdowns of the old and energy-inefficient boilers and kilns reduced the fossil fuel consumption and the emission factors of the residential sectors, as provided in Table S3 in the supplement. Based on the satellite detection in our recent study (Yang and Zhao, 2019), the biomass burning activities in Nanjing were significantly reduced during the period as well, attributed to the gradual prohibition of crop residual burning in the open field.

2.2. Air quality modeling

We applied the Models-3 Community Multi-scale Air Quality (CMAQ) v4.7.1 to evaluate the city-scale emission inventory and the role of emissions on aerosol pollution for Nanjing. As shown in Fig. 1, three nested domains were adopted with the spatial resolutions at 27, 9 and 3 km respectively in the Lambert Conformal Conic projection centered at (110°E, 34°N). The mother domain (D1, 177 × 127 cells) covered most of China, Japan, North and South Korea, while the second (D2, 118 × 121 cells) and third domain (D3, 79 × 91 cells) covered the whole YRD region and Nanjing, respectively. Clean air was set as the background field of D1, and the boundary conditions of D2 and D3 were provided with the simulations of upper domains D1 and D2, respectively. The emissions of anthropogenic origin in D1 and D2 were obtained from the Multi Resolution Emission Inventory for China 2012 (MEIC, http://www.meicmodel.org/) with an original spatial resolution of 0.1°×0.1°. The gridded MEIC emissions were aggregated to 27 km for D1, and were downscaled to 9 km for D2 according to the spatial distributions of population (for residential sources) and gross domestic product (for other sources). The anthropogenic emissions in Nanjing obtained in Section 2.1 were applied for D3. The model configuration on other types of emissions and chemistry mechanisms were described in Zhou et al. (2017). The starting and ending years of the research period, i.e., 2012 and 2016, were selected to conduct the air quality modeling, and January, April, July and October were selected to represent the typical meteorology in winter, spring, summer, and autumn, respectively. A 5-day spin-up period of each month was used to minimize the influences of initial conditions in the simulations.

Meteorological fields were created by simulations of the Weather Research and Forecasting (WRF) version 3.4. The U.S. Geological Survey database was adopted as terrain and land-use data, and the first guess field of meteorological modeling was provided by the final analysis dataset (ds083.2) from National Centers for Environmental Prediction. To evaluate the performance of meteorology modeling, WRF simulated results were compared with the observation dataset of US National Climate Data Center (NCDC) at the Lukou Airport Station in Nanjing.

2.3. Satellite and ground observation

The tropospheric vertical column densities (VCDs) of NO_2 from Ozone Monitoring Instrument (OMI) were applied to test the inter-annual variability of NO_X emissions. Onboard the Aura satellite, OMI has a local time of crossing the equator at 1:30 p.m., and its spatial resolution is 24 × 13 km at nadir. We selected the satellite-derived NO_2 VCDs, as the uncertainty from satellite observation was relatively small for NO_2 compared to other species, and relatively good consistency between the satellite and ground observation was achieved for NO_2 (Liu et al., 2016, 2019bib_Liu_et_al_2016bib_Liu_et_al_2019). In this work, we applied the Dutch Ozone Monitoring Instrument NO_2 (DOMINOv2) product retrieved by KNMI/NASA (Boersma et al., 2011; available at http://www.temis.nl/airpollution/no2.html) to estimate the NO_2 VCDs from 2012 to 2016 for Nanjing based on the monthly data with horizontal resolution of 0.125° × 0.125°. Given the different NO_X emission levels, NO_2 chemistry and meteorology by season, there is usually a clear seasonal variability in the NO_2 VCDs from satellite observation in eastern China, i.e., higher in winter and lower in summer. To eliminate such seasonal variability and to better present the inter-annual change, the 12-month moving average of NO_2 VCDs for each month was calculated as the means of the data for the previous and subsequent six months, and was then compared with the annual estimates of NO_X emissions in this work.

The hourly SO_2, NO_2 and $PM_{2.5}$ concentrations from ground observation for January, April, July and October in 2012 and 2016 were obtained from China National Environmental Monitoring Center (http://www.cnemc.cn/) to evaluate the performance of air quality modeling. As labeled in Fig. 1b, totally nine state-operated monitoring sites were available in Nanjing including six urban sites (Zhonghuamen (ZHM), Xuanwumen (XWM), Shanxilu (SXL), Ruijinlu (RJL), Caochangmen (CCM), and Maigaoqiao (MGQ)), and three suburban sites (Xianlin (XLS), Pukou (PKS), and Olympic Sports Center (OSC)). Due to the incomplete system at the beginning of data reporting of national air quality monitoring in 2012, the hourly concentrations for 2012 were

only available at CCM for January and ZHM and XLS for all the selected month, while those for 2016 were available at all the nine sites. To further check the model performance on the chemical composition of aerosols, the on-line measurement data of sulfate, nitrate, ammonium (SO_4^{2-}, NO_3^- and NH_4^+, SNA), and black carbon (BC) concentrations in $PM_{2.5}$ were obtained at a comprehensive Station for Observing Regional Processes of the Earth System (SORPES) located in east Nanjing (Ding et al., 2013, 2019bib_Ding_et_al_2013bib_Ding_et_al_2019). The inorganic water-soluble ions and BC were measured with the Monitor for AeRosols and GAses in ambient Air (MARGA; Metrohm, Switzerland) and seven-wavelength aethalometer (AE-31, Magee Scientific), respectively, and the daily concentrations were available for the four simulation months, i.e., January, April, July and October 2016 (Ding et al., 2019). The correlation coefficients (R), normalized mean biases (NMB) and normalized mean errors (NME) between the observed and simulated concentrations were calculated by species and site for the simulation periods with the following equations:

$$R_j = \frac{\sum_{i=1}^{n}\left(P_i - \overline{P}\right)\left(O_i - \overline{O}\right)}{\sqrt{\sum_{i=1}^{n}\left(P_i - \overline{P}\right)}\sqrt{\sum_{i=1}^{n}\left(O_i - \overline{O}\right)}} \times 100\% \quad (2)$$

$$NMB_j = \frac{\sum_{i=1}^{n}(P_i - O_i)}{\sum_{i=1}^{n} O_i} \times 100\% \quad (3)$$

$$NME_j = \frac{\sum_{i=1}^{n}|P_i - O_i|}{\sum_{i=1}^{n} O_i} \times 100\% \quad (4)$$

where j represents the species; P and O indicate the hourly (for SO_2, NO_2 and $PM_{2.5}$) or daily concentrations (for chemistry components of $PM_{2.5}$) from modeling prediction and observation, respectively; and $\overline{P}$ and $\overline{O}$ indicate the average of P and O, respectively.

2.4. Evaluation of the roles of emissions and meteorology

To assess the roles of the changed emissions and meteorological conditions on the inter-annual variation of $PM_{2.5}$ concentrations in Nanjing, we performed the CMAQ simulation for 2012, and three simulations including SBOTH, SMETEO and SEMISS for 2016. As an estimation of reality, SBOTH is a simulation of $PM_{2.5}$ concentrations with both meteorological conditions and anthropogenic emissions set at the 2016 level. SMETEO is a simulation with the meteorological conditions at the 2016 level and the fixed anthropogenic emissions in Nanjing at 2012. It can thus quantify the impact of varied meteorology on the ambient $PM_{2.5}$ levels alone for the city during the research period. In contrast, SEMISS is a simulation with the anthropogenic emissions in Nanjing at the 2016 level and the fixed meteorological condition at 2012. It reflected the impact of varied anthropogenic emissions alone on the ambient $PM_{2.5}$ levels. In SBOTH and SEMISS simulations, moreover, the declining rates of anthropogenic emissions outside Nanjing in D3 were assumed to be the same as those for Nanjing, attributed mainly to the lack of detailed emission controls in the areas surrounding Nanjing for the research period in this work.

3. Results and discussions

3.1. The city-level emissions from 2012 to 2016

Summarized in Table 1 are the annual emissions of selected air pollutants for Nanjing from 2012 to 2016 estimated in this study. Due to the improved controls mentioned in Section 2.1, clear reduction was found for most species. The emissions of SO_2, CO, NH_3, $PM_{2.5}$, BC, and OC declined by 70%, 49%, 72%, 64%, 65%, and 86%, respectively. Compared to other gaseous species and particles, less benefit was found for NOx with its emissions reduced 22%, while slight increase was even estimated for the VOCs emissions during the period. Quantification of the uncertainty of emission estimation could be challenging, particularly at city scale with insufficient statistics and domestic measurements. In our previous study, we improved a methodology of Mont-Carlo simulation and quantified the uncertainty of Nanjing's power plus industrial emissions at -17-22%, -10-33%, -23-75%, -28-48%, -45-82%, and -34-96% (95% confidence interval) for SO_2, NO_X, CO, $PM_{2.5}$, BC, and OC in 2012, respectively (Zhao et al., 2017b). Little improvement in the uncertainty analysis was achieved for other sectors compared to the national level (Zhao et al., 2011) due to the limited progress in data collection.

Table 2 provides the emissions with their relative changes from 2012 to 2016 by source category. For the power sector, the largest reduction in emissions was found for SO_2, while those for NO_2 and primary $PM_{2.5}$ were smaller. Based on the detailed statistics on individual plants, the annual coal consumption of the sector reduced 10%, from 18.7 million metric tons to 16.7 during the research period, attributed to the adjustment in energy structure by local government. As indicated in Table S1, the removal efficiencies of flue gas desulfurization (FGD) systems for the main plants in Nanjing were increased, leading to considerable benefits of SO_2 control. Although the penetration and operation of selective catalyst reduction (SCR) systems on coal-fired power sectors were improved, the NO_X emissions did not decline as much as SO_2. As the government implemented the switch from coal use to gas and oil for the power sector, the penetration of oil and gas-fired units were enhanced, but the emission controls for them were not as

Table 2
The changes in annual emissions between 2012 and 2016 by sector. To ease comparison, the value for industry VOCs in the table contains emissions from both industry and solvent use sources.

		SO_2	NO_X	$PM_{2.5}$	VOCs
Industry	2012 (tons)	70,701	53,708	62,813	131,940
	2016 (tons)	21,250	42,225	18,095	156,954
	Relative change	−70%	−21%	−71%	19%
Power	2012 (tons)	59,374	93,982	8938	1139
	2016 (tons)	16,421	65,370	6912	1114
	Relative change	−72%	−30%	−23%	−2%
Residential	2012 (tons)	6670	3342	4524	5449
	2016 (tons)	1530	1428	219	286
	Relative change	−77%	−57%	−95%	−94%
Transportation	2012 (tons)	3925	58,773	3724	17,152
	2016 (tons)	2789	54,290	1923	18,924
	Relative change	−29%	−8%	−48%	10%

Table 1
The annual emissions of typical air pollutants from 2012 to 2016 in Nanjing (unit: tons).

	SO_2	NO_X	CO	NH_3	VOC	$PM_{2.5}$	BC	OC
2012	140,670	209,805	743,000	64,000	155,680	79,999	5835	7138
2013	90,908	194,544	583,700	48,730	198,078	68,739	5819	6295
2014	82,800	182,100	472,000	27,600	206,900	62,542	3700	5200
2015	45,986	176,795	416,698	25,400	174,177	32,266	2309	1117
2016	41,991	163,313	378,232	17,459	177,278	27,149	2044	953

strict as coal-fired units. The benefits of NO_X emission control on coal-fired units were thus weakened. Similarly, the city has been conducting comprehensive retrofitting on coal-fired boilers in the industry sector and has gradually shut down small iron & steel and cement production plants since 2012. Almost all of the coal-fired boilers had been closed or switched to oil/gas-fired ones by 2016. As a result, the SO_2 and $PM_{2.5}$ emissions from industrial sources significantly declined (over 70% for both species) during 2012–2016, while NO_X emissions were reduced less. The huge reduction in emissions from residential and commercial sources was achieved during the research period, attributed mainly to three approaches. The first was the retrofitting or shutting down the coal-fired boilers for commercial use, similar with the industry sector; the second was the eliminating of coal stoves or switching them to gas stoves for household use; and the third was the prohibition of biomass open burning. For the transportation sector, the implementation of staged emission standards overwhelmed the increased population of diesel vehicles and engines, and thereby reduced the emissions of NO_X and $PM_{2.5}$. In particular, the benefits of NO_X control was less than other species, as recent on-road measurements indicated that some vehicles labeled with Stage IV (equal to Euro IV) or stricter standard failed to meet the requirement of emission limit and thus had emission factors larger than expected (Wu et al., 2012). Industry and solvent use were estimated to account collectively for nearly 80% of anthropogenic VOCs emissions in Nanjing. In contrast to SO_2 and NO_X for which the control started before 2012, there were still limited measures and technologies on VOCs reduction for chemical industry and refinery plants. Besides stack emissions, considerable fugitive emissions were expected from those plants attributed to miscellaneous procedures that were not effectively monitored. Moreover, the VOCs emissions from transportation were estimated to grow as well, resulting from the swift increase in gasoline passenger cars in the city. Agricultural activities dominated the NH_3 emissions. The fast urbanization largely reduced the livestock farming and became the main driving force of a large decrease in NH_3 emissions.

Fig. S2 in the supplement illustrates the spatial distribution of emissions for selected pollutants in Nanjing 2016. As can be seen in the figure, the spatial distributions of most species were largely influenced by locations of individual plants. The pattern implies that big point sources in Nanjing dominated the emissions along with the retirement of small and old plants. For BC and OC that are more related to residential and household activities, more emissions were found in urban areas attributed to the large population density.

3.2. Evaluation of city-scale emissions with observation and AQM

3.2.1. Satellite observation of NO_2 tropospheric VCDs

Fig. 2 illustrates the inter-annual variabilities in the NO_2 tropospheric VCDs from 2006 to 2016 and that in the bottom-up estimation of NO_X emissions from 2010 to 2016 in Nanjing. The emissions for 2010 and 2011 were taken from our previous study (Zhao et al., 2015) while those for the remaining years were from this work. The NO_2 VCDs for the whole YRD region and its biggest city, Shanghai, were provided in the figure as well for comparison. All the data are normalized to the 2010 level in Nanjing, thus the relative changes to 2010 are revealed instead of the absolute magnitudes for VCDs or emissions.

As shown in the figure, the NO_2 VCDs in megacities (Nanjing and Shanghai) remained higher than the regional average, indicating the large emission intensities in cities with large population and developed economy for the past ten years. Emission control policies were first put into effect in megacities. This included implementation of staged emission standards for on-road vehicles, and old and inefficient coal-fired boilers being closed or moved to suburban areas. As indicated in Fig. 2, the NO_2 VCDs in Shanghai stopped growing and started to decline around 2008, and the gap of NO_2 VCDs between Shanghai and other regions in YRD were clearly reduced for recent years. As a comparison, the NO_2 VCDs for Nanjing (and other YRD regions) kept growing until 2011, implying a slower progress in NO_X control than Shanghai. The bottom-up estimation in this work revealed the peak of NO_X emissions for Nanjing in 2012, and the inter-annual change in the city emissions closely matched that in NO_2 VCDs for recent years. The consistency between the relative inter-annual changes in emissions (the pink triangles in Fig. 2) and VCDs (the blue line in Fig. 2) implies the reasonable temporal variability of city-level NO_X emissions in our bottom-up inventory and the benefit of emission control for the city.

Uncertainty should be noted in this direct comparison between emissions and VCDs. Besides the uncertainty from emission estimation as mentioned in Section 3.1, the bias in retrieval from satellite observations is always a concern when used in evaluation of atmospheric compositions. In particular, the sensitivity of satellite detection declines towards the surface, and uncertainty is introduced when applying the

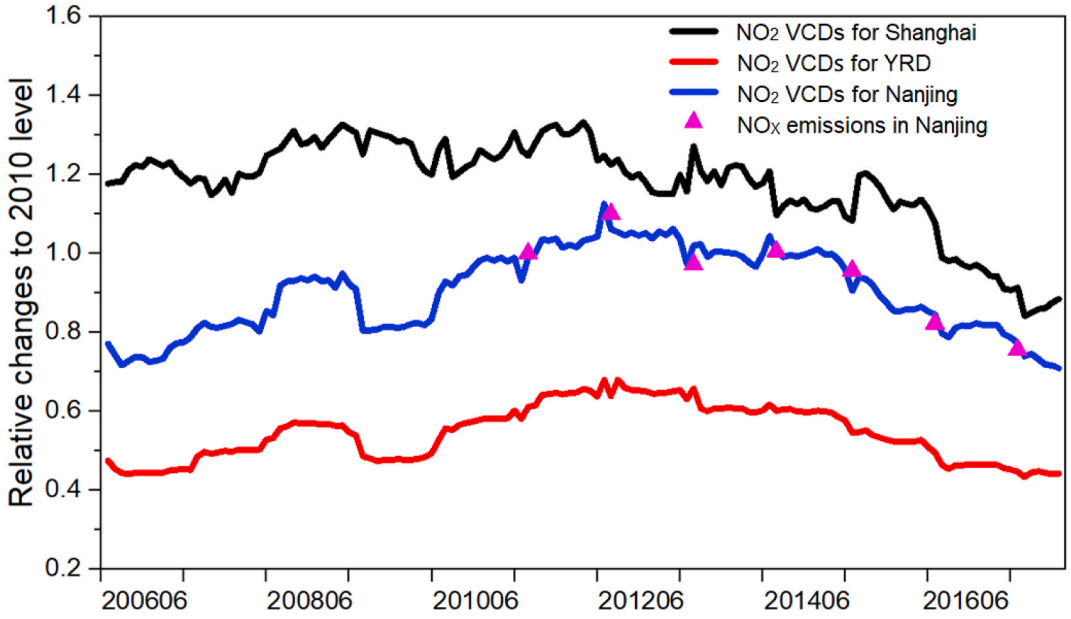

Fig. 2. The inter-annual changes in NO_2 vertical column density (VCD) 2006–2016 for selected YRD regions and those in bottom-up NO_X emissions for 2010–2016 for Nanjing. All the data are normalized to 2010 level in Nanjing.

total columns in the troposphere for evaluating the anthropogenic emissions released from the surface. For example, Boersma et al. (2016) found the error of vertical sampling in satellite retrieval reached 20% through comparison between the OMI-derived and simulated NO_2 using a global model, GEOS-Chem. Therefore, the good agreement found in this work for Nanjing should be interpreted cautiously. Given the relatively small spatial coverage for cities and relatively coarse horizontal resolution of satellite detection, moreover, OMI was expected to be less effective in constraining the emission pattern at city-scale than the regional scale (Yang et al., 2019). Along with the increased use in satellite products with elevated resolution (e.g., those from TROPOMI launched at the end of 2017), a more reasonable assessment of city-level emission studies could be achieved in future.

3.3. AQM for regulated air pollutants

Table S4 and Fig. S3 in the supplement provide the comparisons between the observed and simulated meteorology parameters with WRF, taking January 2012 as an example. In general, the simulated wind speed, wind direction, relative humidity and temperature for D3 were consistent with the observation and the simulation was in compliance with the benchmarks derived from Emery et al. (2001) and

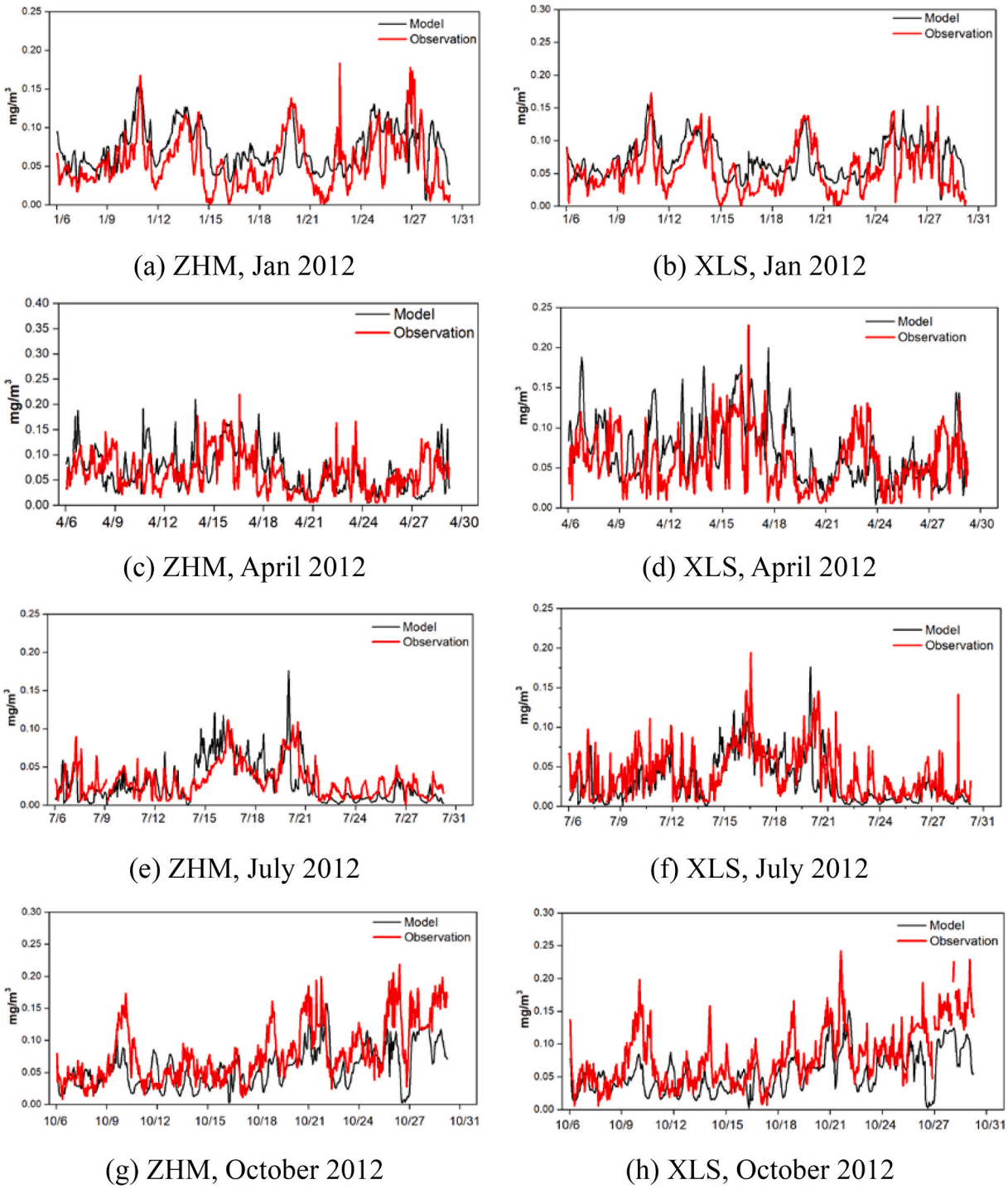

Fig. 3. The simulated and observed $PM_{2.5}$ concentrations at ZHM and XLS for January, April, July, and October 2012.

Jiménez et al. (2006). The average bias and the root mean squared error (RMSE) between the simulated and observed wind speed were 0.76 and 1.56 m/s, respectively, and the index of agreement (IOA) reached 0.71. The average bias for the wind direction was 3.4°, smaller than the benchmark at 10°. The average biases for temperature and relative humidity were 0.49 °C and 5.1, and IOAs were both above than 0.9.

The hourly concentrations of SO_2, NO_2 and $PM_{2.5}$ simulated with CMAQ for 2012 and 2016 in Nanjing were compared against the observations at the nine state-operated air quality monitoring stations. The NMBs and NMEs between the simulated and observed concentrations are summarized in Table S5 in the supplement by month and pollutant, based on the aggregated site-specific information. Most NMBs and NMEs are smaller than 20% and 50%, respectively, indicating the reliability of CMAQ modeling. The comparison between simulation and observation suggests the reasonable estimation in the magnitude and seasonal distribution of air pollution emissions, and implies that the current emission inventory was suitable for the AQM purpose at the city scale. For the primary pollutants SO_2 and NO_X, the AQM slightly overestimated the concentrations indicated by the positive NMBs in most case for 2012. Besides the uncertainty of the AQM itself, the positive bias could be due to elevated emissions estimated in the bottom-up inventory stemming from not fully capturing the emission control measures in earlier years.

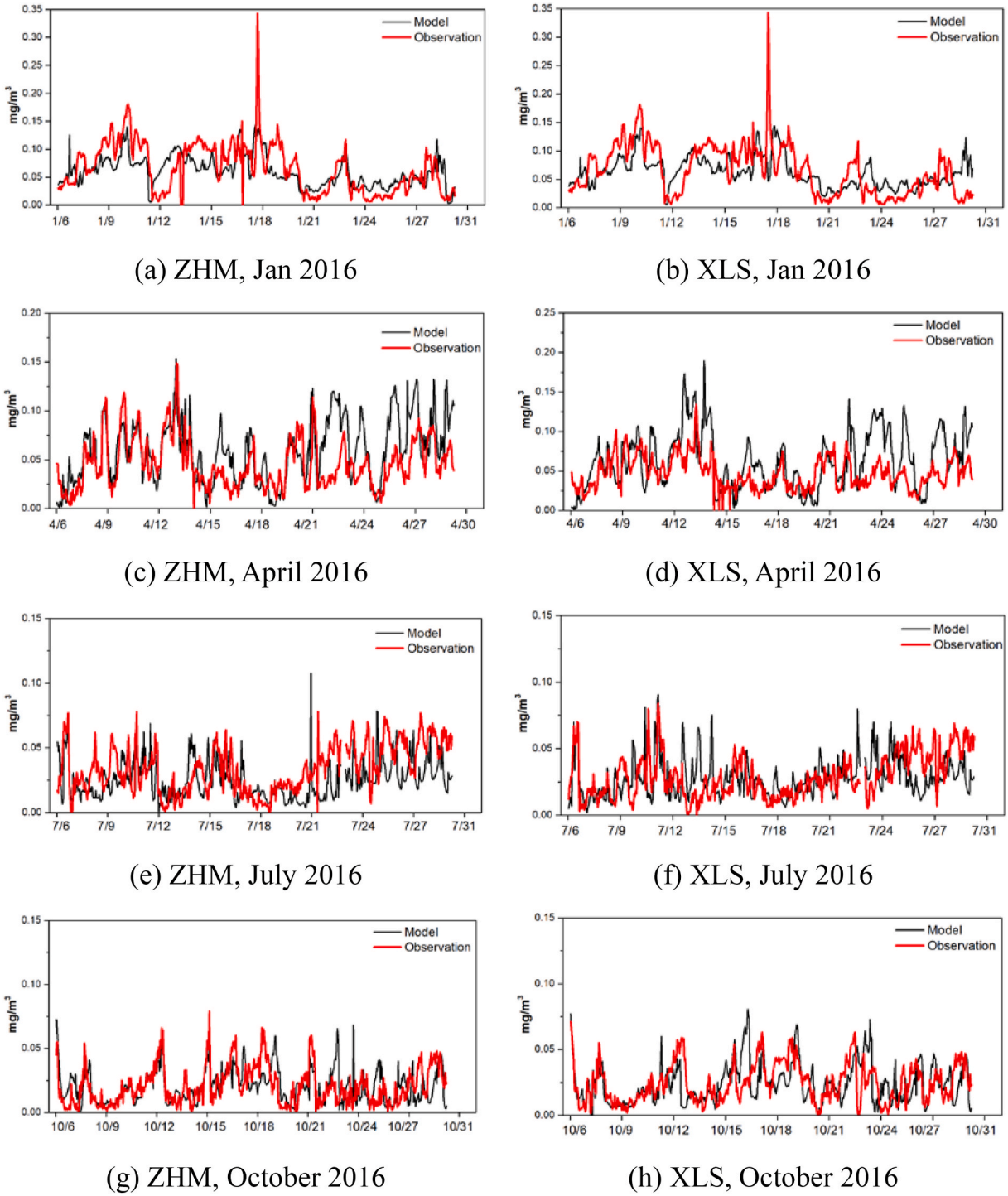

Fig. 4. The same as Fig. 3 but for 2016.

This bias was partly corrected for 2016, as the implemented measures were gradually considered in the emission estimation. The large NMEs were generally found for $PM_{2.5}$ that comes both from primary emissions and secondary formation. The result implies the limitation in PM formation mechanism of CMAQ 4.7.1. The more recent version CMAQ 5.1 with the newly added subdivision of emission species and mechanism of secondary aerosol formation was demonstrated to be able to improve the $PM_{2.5}$ simulation in the YRD region (Lu et al., 2020). Suggested by the larger correlation coefficients (R in Table S5) for $PM_{2.5}$ than SO_2 or NO_2, the model could better capture the temporal variation of $PM_{2.5}$ concentration than those of primary pollutants. As the changes in local emissions might not be fully considered in bottom-up inventory, larger bias can be expected in the simulation of SO_2 and NO_2 that are more dependent on emissions. In contrast, as secondary formation played an important role in $PM_{2.5}$ mass concentrations, the misspecification of emissions in the bottom-up inventory were expected to have less influence on $PM_{2.5}$ levels compared to SO_2 and NO_2.

Site-specific modeling performance was further explored. Taking an urban (ZHM) and suburban site (XLS) for example, Figs. 3 and 4 illustrate the time-series of simulated and observed hourly concentrations of $PM_{2.5}$ for the two years, respectively. The results of the remaining seven sites for 2016 are provided by month in Figs. S4–S7 in the supplement. In general, CMAQ modeling could capture the peaks and drops of $PM_{2.5}$ concentrations in most cases, and reproduced the time-series of $PM_{2.5}$ concentrations in both urban and suburban areas. Some extremely high concentrations were simulated, attributed possibly to the uncertainty in meteorology simulation. In late April 2016, for example, WRF provided clearly higher relative humidity and smaller wind speed than the observation for 23–25 April (Fig. S8 in the supplement), leading to the overestimation in $PM_{2.5}$ concentrations at most sites (Fig. S5). Table S6 in the supplement summarizes the model performance statistics by month and site for 2016. The NMB, NME and R for all of the four months were ranged −15%~5%, 36%~46%, and 0.48–0.57 among the nine sites, respectively. It can be found that the difference in model performance between the suburban (OSC, XLS, and PKS) and urban sites (the remaining ones) was insignificant. On one hand, the city-scale emission inventory improved the spatial allocation of primary emissions and could thereby partly correct the overestimation in air pollutant concentrations for the urban areas based on the national emission data (Zhou et al., 2017). On the other hand, given the relatively close distance between each other, the urban and suburban sites were influenced by similar processes of particle emissions and formation. The aging of aerosols was less effective than it was supposed to be in the more remote areas. When available, information at background sites of the city could further help understand the spatial pattern of ambient $PM_{2.5}$.

3.2.3. AQM for chemistry components of $PM_{2.5}$

Fig. 5 illustrates the simulated and observed concentrations of SO_4^{2-}, NO_3^-, NH_4^+, and BC in $PM_{2.5}$ at SORPES for the four months in 2016, and the NMEs, NMBs and R between simulation and observation are summarized in Table 3. The model performed well in predicting the concentrations at monthly average with slight underestimation, indicated by the small NMBs (less than 15% for all the species). The NMEs were larger, implying the bigger uncertainty in the simulation of time-series of particle component concentrations, particularly for NO_3^- and NH_4^+ with the NMEs estimated at 56% and 46%, respectively. As shown in Fig. 5, clear overestimation was found for April and underestimation was found for July for the two species. As a comparison, we conducted CMAQ simulation of SNA for the whole YRD region in our previous study (Zhao et al., 2020). As summarized in Table 3 the monthly NMEs between observation and simulation were ranged 42–110%, 45%–143%, and 40–100% for SO_4^{2-}, NO_3^-, and NH_4^+, respectively, based on available two monitoring sites in the region (SHPD in Shanghai and JSPAES in Jiangsu). Comparing the NMBs and NMEs in Table 3, the modeling error for Nanjing in this work was clearly reduced, suggesting the improvement of emission inventory at the city scale. For all the species included

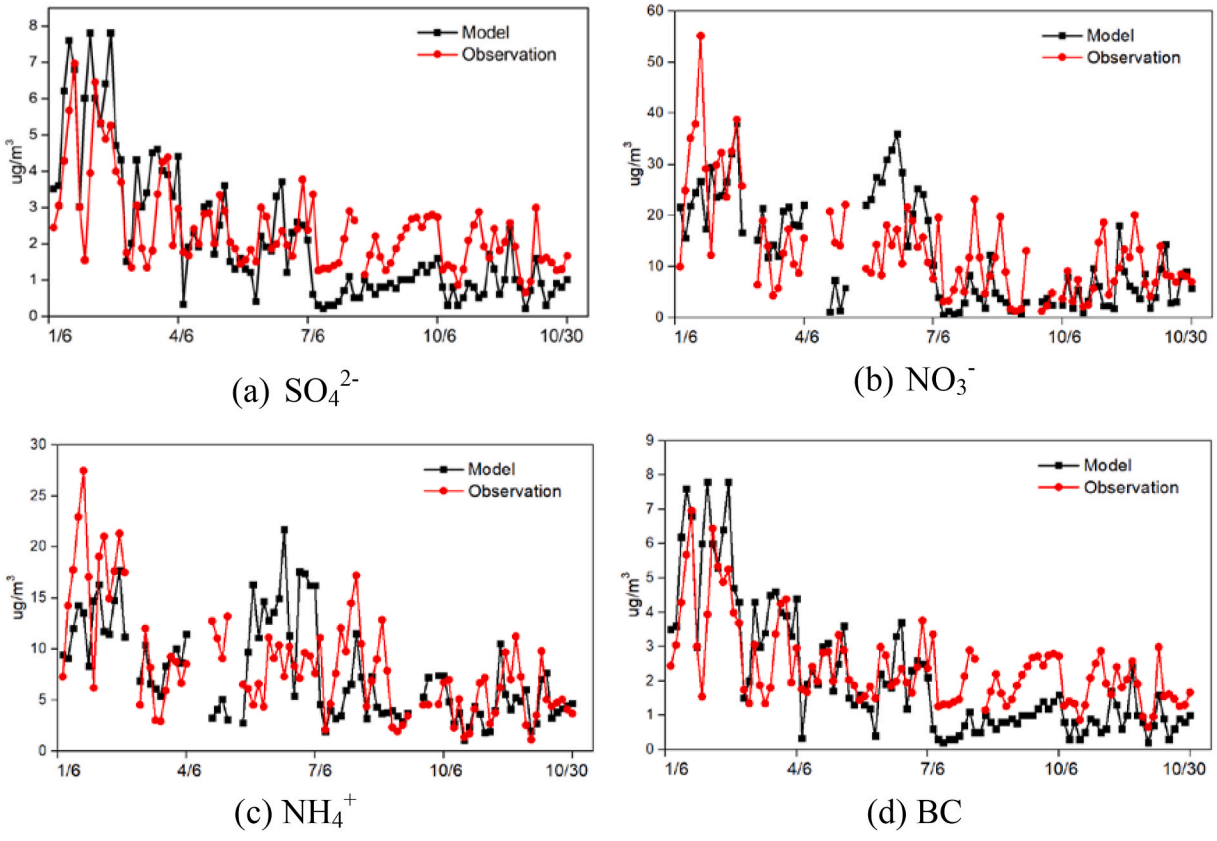

Fig. 5. The concentrations of SO_4^{2-} (a), NO_3^- (b), NH_4^+ (c) and BC (d) from observation and CMAQ simulation at SORPES for January, April, July, and October 2016.

Table 3
Model performance statistics for concentrations of SO_4^{2-}, NO_3^-, NH_4^+ and BC at SORPES. n indicates the sample size of daily concentrations. The model performance based on the regional-scale emission inventory for another two YRD sites is taken from Zhao et al. (2020) and provided as well for comparison.

	SO_4^{2-}	NO_3^-	NH_4^+	BC
SORPES (this work)				
NMB	−14%	−7%	−8%	−11%
NME	34%	56%	46%	41%
R	0.55	0.55	0.49	0.77
n	100	89	90	100
SHPD and JSPAES [a]				
NMB	14–92%	−78–29%	−19–84%	N/A
NME	42–110%	45–143%	40–100%	N/A
R	0.34–0.55	0.49–0.62	0.56–0.66	N/A

[a] The results at the two sites are taken from Zhao et al. (2020). SHPD is a suburban site in Pudong, Shanghai, and JSPAES is an urban site in Nanjing. The statistics were based on the hourly concentrations from ground observation with MARGA and CMAQ modeling for April and July 2014 at SHPD and October 2014 at both SHPD and JSPAES.

in Table 3, the strongest temporal correlation between the observation and simulation was found for BC, the species inactive in chemistry. Due to the limited availability of continuous measurement data of aerosol species, the evaluation of AQM on aerosol species based on the city-scale emission data was an initiated step and could be further improved when more reliable observation data become available.

3.3. Role of the emission control and meteorology on the changed $PM_{2.5}$ level

3.3.1. Contribution from reduced emissions and varied meteorology

Fig. 6 illustrates the monthly $PM_{2.5}$ concentrations for 2012 and 2016 obtained from both ground observation and various CMAQ simulations as described in Section 2.4, and the relative changes between the two years are summarized in Table 4. Both the observation and AQM (SBOTH) found clear abatement in ambient $PM_{2.5}$ concentrations from 2012 to 2016 for all the concerned months except January, with the smallest reduction rate in April and the largest in October. The reduction rates from simulation were generally smaller than those from observation. In particular, observation and AQM suggested that the $PM_{2.5}$ concentrations of October in Nanjing declined 71% and 60%, respectively, indicating that the alleviated aerosol pollution for recent years in Nanjing could be effectively captured by the model in specific seasons. Different from the remaining three months, there is a clear contradiction

Table 4
Changes in $PM_{2.5}$ concentrations in January, April, July and October between 2012 and 2016 for SBOTH, SMETEO and SEMISS simulations and observation. n indicates the sample size of AQM (i.e., the number of grids within Nanjing in D3).

	January	April	July	October
SBOTH	−29%	−8%	−10%	−60%
SMETEO	−21%	5%	−3%	−37%
SEMISS	−16%	−22%	−5%	−18%
Observation	33%	−18%	−28%	−71%
n	844	844	844	844

in the relative change of $PM_{2.5}$ between measurement and simulation for January. Ground observation found the $PM_{2.5}$ concentration increased 33% while the AQM suggested it declined 29%. The disagreement could result both from the meteorology simulation and bias in emission estimation. As shown in Table S7 in the supplement, increased wind speed and precipitation, as well as decreased relative humidity were simulated for January from 2012 to 2016. Such changes were expected to reduce the $PM_{2.5}$ concentrations. Regarding the emission data, moreover, the household emissions were expected to largely decline attributed to shutdowns of old and small kilns and thereby less fossil fuel use, as mentioned in Section 2.1. This estimation, however, could be too optimistic in winter. Although there was no central heating in Nanjing, fossil fuel was used for household heating. Such consumption was hardly recorded in official statistics and did not necessarily decline significantly during the research period. Therefore, the emissions in winter might not have reduced as fast as estimated in the current bottom-up inventory. In a summary, the $PM_{2.5}$ concentration in Nanjing was estimated to decline 28% from 2012 to 2016, based on the averages of simulated monthly values for January, April, July and October, while the analogue number for ground observation was 25%. As a comparison, the primary $PM_{2.5}$ emissions were estimated to decline 64% during the period in the city-level emission inventory. The much smaller reduction in ambient level than the primary emissions of $PM_{2.5}$ suggested the strong nonlinearity of $PM_{2.5}$ formation. Regarding the precursors involved in the secondary aerosol formation, SO_2, NO_X, and NH_3 were estimated to reduce 22%–72%, while VOC increased, as mentioned in Section 3.1. The heterogeneity of emission variations for those precursors is a great reason for the nonlinearity of $PM_{2.5}$ reduction. For better understanding the response of ambient $PM_{2.5}$ level to precursor emission changes, multiple-year observation of certain aerosol chemistry components related to precursors is recommended including SO_4^{2-}, NO_3^- and OC.

Given the relatively large uncertainty in the simulation of inter-

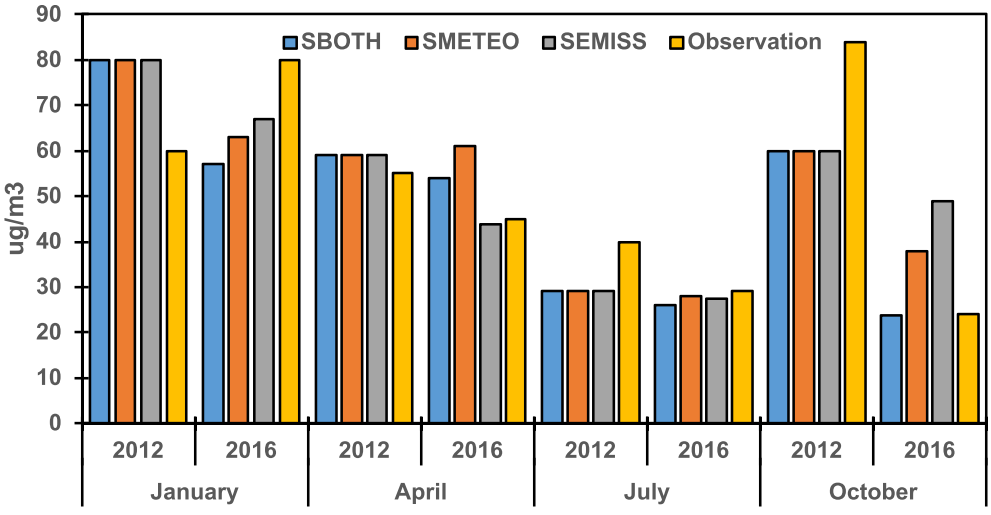

Fig. 6. The observed and simulated monthly mean of $PM_{2.5}$ concentrations in SBOTH, SMETEO and SEMISS for January, April, July and October of 2012 and 2016 in Nanjing.

annual changes in $PM_{2.5}$ concentrations for January, we compared the results of SBOTH, SMETEO and SEMISS simulations for April, July and October to understand the roles of emissions and meteorology on the varied $PM_{2.5}$ concentrations. As an average of the three months, $PM_{2.5}$ concentration was simulated to reduce 28% between 2012 and 2016 (SBOTH). As shown in Fig. 6 and Table 4, the $PM_{2.5}$ concentration over Nanjing in April 2016 was elevated by 5% compared to that in 2012 in SMETEO simulation, while it decreased 22% in SEMISS. The result thus implies a greater impact of the reduced emissions on aerosol pollution alleviation than the changed meteorology. The combined effect of emission and meteorology changes led to 8% reduction in $PM_{2.5}$ concentrations, as indicated in SBOTH. The meteorology conditions in July for the two years was similar and had little effect on $PM_{2.5}$ variation, and the reduced emissions resulted in a 5% reduction of $PM_{2.5}$. In October, the changed meteorology conditions and emissions were estimated to result in 37% (SMETEO) and 18% (SEMISS) reduction of $PM_{2.5}$ concentration, respectively, and the result indicates that meteorology played a more important role on reduced aerosol pollution for the month. The more important role of meteorology in October can be further supported by a correlation analysis between the changes in simulated $PM_{2.5}$ concentrations and individual meteorology factors, as presented in Table S8 in the supplement. Compared to other months, very high coefficients were found between $PM_{2.5}$ and all the selected meteorology factors in October.

Limitation should be acknowledged in separating the roles of emissions and meteorology on $PM_{2.5}$ pollution. The varied meteorology influences specific human activities, and thereby changes the air pollutant emissions of anthropogenic sources. Such interaction between meteorology and human activities was not sufficiently considered in current emission inventory development. For example, the emissions from on-road vehicles were calculated using the meteorology parameters as correction factors (Huang et al., 2017). For power sector, however, the daily variation from the on-line emission measurement was not incorporated in the inventory, and its correlation with daily meteorology that influences the electricity demand was not analyzed yet. The impacts of meteorology on NH_3 volatilization for the YRD region (Zhao et al., 2020) have not been applied for emission estimation for continuous years in this study either. Therefore, uncertainty existed in the analysis of the contributions of emission and meteorology changes to the reduced $PM_{2.5}$ levels.

3.3.2. *Effects of sectoral emissions on reduced $PM_{2.5}$ concentration*

To detect the contribution of individual sectors to the reduced $PM_{2.5}$ concentrations, a sensitivity analysis was further conducted on top of SEMISS simulation. In this extra simulation, the emissions from industry, power, transportation, and residential sectors for 2012 were replaced with those for 2016, respectively, while the emissions for the remaining sources and the meteorology inputs were fixed at the 2012 level. The spatial distributions of $PM_{2.5}$ concentrations of the extra simulation are illustrated in Fig. 7, as well as those of SBOTH and

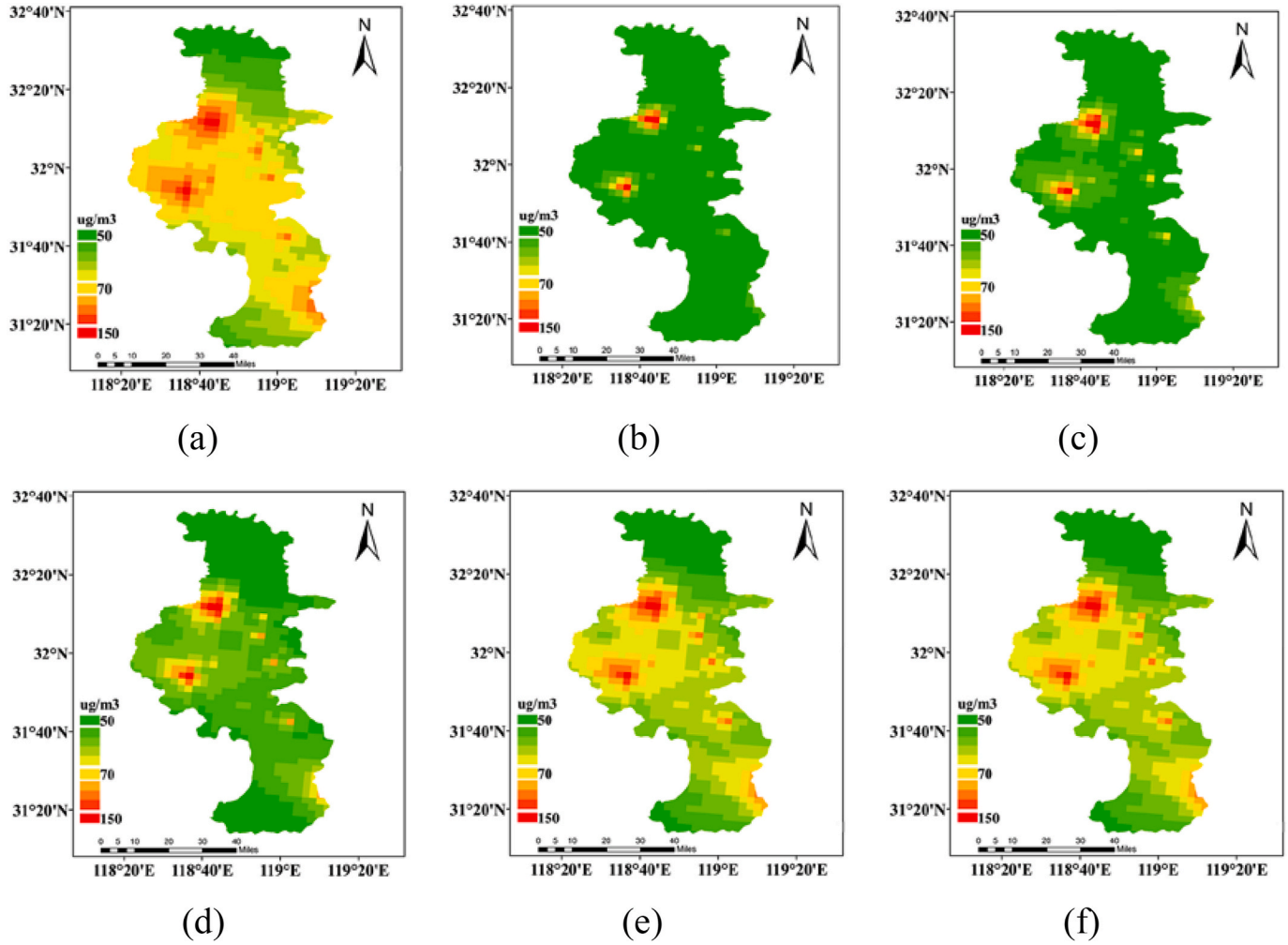

Fig. 7. The spatial distributions of the simulated $PM_{2.5}$ concentrations (the average of January, April, July and October) in Nanjing under the 2012 meteorology condition. Panel (a) is the case with the emission data for 2012 applied. Panels (b)–(f) are the cases in which the emissions from all the anthropogenic, industrial, power, transportation, and residential sources were replaced with the 2016 data, respectively.

SEMISS for 2012. Compared to Fig. 7a, the simulated $PM_{2.5}$ concentrations overall Nanjing were reduced −17%, −12%, −5%, and −5%, respectively for Fig. 7c, d, 7e, and 7f. The effective control on industrial emissions was thus expected as the biggest driving force of $PM_{2.5}$ abatement for the recent years, followed by power, transportation and residential sources. As summarized in Tables 1 and 2, the annual emissions of anthropogenic SO_2, NO_X and primary PM emissions of anthropogenic origin were reduced by 98.7, 46.5 and 52.8 kilo metric tons, and industrial sector was estimated to contribute 50%, 25% and 85% to the emission abatement, respectively. The analogue numbers for power sector reached 44%, 62% and 4%, respectively. Therefore, the industrial and power sectors dominated the emission abatement for the research period. Given the high stacks of power plants and thereby relatively long-range transport of pollutants, less benefit of emission control on local power sector was found for the city. Although the relative changes in annual emissions of transportation and residential sources were large as well (Table 2), they were found to play a less important role in aerosol pollution reduction during the research period as their contributions to total annual emissions in the city were small, with an exception of NO_X from transportation.

4. Conclusion

Taking Nanjing as an example of developed cities in east China, this work quantified the inter-annual changes in air pollutant emissions and evaluated the roles of variation in emissions and meteorology on the reduced aerosol pollution in recent years. From 2012 to 2016, over 60% of annual emission abatement was achieved for SO_2 and primary particles reflecting the impacts of national and local policies of air pollution control, while the reduction rate for NO_X was smaller at 22%. The inter-annual variation in NO_X emissions were clearly supported by satellite observation. Based on the available ground observation, the reliability of this city-scale emission inventory was further evaluated through AQM, and satisfying agreement between simulation and observation was achieved for both regulated pollutants (SO_2, NO_2 and $PM_{2.5}$) and selected $PM_{2.5}$ components. The AQM suggested a 28% reduction of $PM_{2.5}$ concentrations 2012 to 2016, based on the average of monthly values for January, April, July, and October, and the result was comparable with that from ground observation at 25%. Based on more simulations with the meteorology or emission input separately fixed at the 2012 level, the reduced anthropogenic emissions from 2012 to 2016 were found to play a more important role on aerosol pollution reduction compared to the changed meteorology in all the selected months except October. Industrial and power sectors were identified as the main contributor of emission abatement and resulting reduced aerosol pollution. In addition to the analysis at the national scale, this study revealed that the effective control on anthropogenic sources (mainly industry and power) was the main driving force of air quality improvement for Nanjing at the city scale. The study could be further improved with additional observation data for evaluation of emission inventories and AQM, including the satellite products with increased horizontal resolution and additional ground measurements of ambient particle species. To better separate the roles of emissions and meteorology on air quality, moreover, more careful analysis on the interaction between human activity and meteorology is recommended.

CRediT authorship contribution statement

Yu Zhao: Conceptualization, Methodology, Resources, Data curation, Writing - original draft. **Yiwei Huang:** Methodology, Investigation, Software, Data curation. **Fangjian Xie:** Resources, Data curation. **Xin Huang:** Resources, Data curation. **Yang Yang:** Data curation.

Declaration of competing interest

The authors declare that they have no known competing financial interests or personal relationships that could have appeared to influence the work reported in this paper.

Acknowledgement

This work was sponsored by Natural Science Foundation of China (91644220 and 41922052) and the National Key Research and Development Program of China (2017YFC0210106). We would like to thank Wenqing Li from Nanjing Bureau of Ecological Environment for technical support of this work, Aijun Ding from Nanjing University for ground observation data, and MEIC (http://www.meicmodel.org/) and TEMIS (http://www.temis.nl/) for free use of the emission and monitoring data.

Appendix A. Supplementary data

Supplementary data to this article can be found online at https://doi.org/10.1016/j.atmosenv.2020.118080.

References

Boersma, K.F., Eskes, H.J., Dirksen, R.J., et al., 2011. An improved tropospheric NO_2 column retrieval algorithm for the Ozone Monitoring Instrument. Atmos. Meas. Tech. 4, 1905–1928.

Boersma, K.F., Vinken, G.C.M., Eskes, H.J., 2016. Representativeness errors in comparing chemistry transport and chemistry climate models with satellite UV–Vis tropospheric column retrievals. Geosci. Model Dev. (GMD) 9, 875–898.

Chen, Y., Schleicher, N., Chen, Y., et al., 2014. The influence of governmental mitigation measures on contamination characteristics of $PM_{2.5}$ in Beijing. Sci. Total Environ. 490, 647–658.

Ding, A., Fu, C., Yang, X., et al., 2013. Ozone and fine particle in the western Yangtze River Delta: an overview of 1-yr data at the SORPES station. Atmos. Chem. Phys. 13, 5813–5830.

Ding, J., Miyazaki, K., van der, A.R.J., et al., 2017. Intercomparison of NO_X emission inventories over east Asia. Atmos. Chem. Phys. 17, 10125–10141.

Ding, A., Huang, X., Nie, W., et al., 2019. Significant reduction of $PM_{2.5}$ in eastern China due to regional-scale emission control: evidence from SORPES in 2011–2018. Atmos. Chem. Phys. 19, 11791–11801.

Emery, C., Tai, E., Yarwood, G., 2001. Enhanced Meteorological Modeling and Performance Evaluation for Two Texas Episodes, Report to the Texas Natural Resources Conservation Commission. International Corp, Novato, CA prepared by ENVIRON.

He, K., Zhao, Q., Ma, Y., et al., 2012. Spatial and seasonal variability of $PM_{2.5}$ acidity at two Chinese megacities: insights into the formation of secondary inorganic aerosols. Atmos. Chem. Phys. 12, 1377–1395.

Huang, Y., Zhao, Y., Yang, Y., et al., 2017. Study on the emission inventory of provincial vehicles based on different methods: a case of Jiangsu Province. China Sci. Pap. 12, 346–353 (in Chinese).

Jiménez, P., Jorba, O., Parra, R., et al., 2006. Evaluation of MM5-EMICAT2000-CMAQ performance and sensitivity in complex terrain: high-resolution application to the northeastern Iberian Peninsula. Atmos. Environ. 40, 5056–5072.

Li, C., McLinden, C., Fioletov, V., et al., 2017. India is overtaking China as the world's largest emitter of anthropogenic sulfur dioxide. Sci. Rep. 7, 14304. https://doi.org/10.1038/s41598-017-14639-8.

Liu, F., Zhang, Q., Ronald, J.V., et al., 2016. Recent reduction in NOx emissions over China: synthesis of satellite observations and emission inventories. Environ. Res. Lett. 11, 114002. https://doi.org/10.1088/1748-9326/11/11/114002.

Liu, M.Y., Lin, J.T., Boersma, K.F., et al., 2019. Improved aerosol correction for OMI tropospheric NO_2 retrieval over East Asia: constraint from CALIOP aerosol vertical profile. Atmos. Meas. Tech. 12, 1–21.

Lou, S., Liao, H., Yang, Y., et al., 2015. Simulation of the interannual variations of tropospheric ozone over China: roles of variations in meteorological parameters and anthropogenic emissions. Atmos. Environ. 122, 839–851.

Lu, Y., Zhao, X., Zhao, Y., 2020. The comparison and evaluation of air pollutant simulation for the Yangtze River Delta region with different versions of air quality model. Environ. Monit. Forewarn. 12 https://doi.org/10.3969/j.issn.1674-6732.2020.03.001 (in Chinese).

Mao, Y.H., Liao, H., Han, Y.M., et al., 2016. Impacts of meteorological parameters and emissions on decadal and interannual variations of black carbon in China for 1980–2010. J. Geophys. Res. 121, 1822–1843.

Ming, L., Jin, L., Li, J., et al., 2017. $PM_{2.5}$ in the Yangtze River Delta, China: chemical compositions, seasonal variations, and regional pollution events. Environ. Pollut. 223, 200–212.

Ministry of Ecology and Environment (Mee), 2018. The communique of Chinese ecological environment status (in Chinese). Available at (last access. http://www.mee.gov.cn/hjzl/zghjzkgb/lnzghjzkgb/. (Accessed 18 January 2020).

Ministry of Environmental Protection (Mep), 2012. China National Ambient Air Quality Standards, GB3095-2012. MEP, Beijing, China (in Chinese).

Mu, Q., Liao, H., 2014. Simulation of the interannual variations of aerosols in China: role of variations in meteorological parameters. Atmos. Chem. Phys. 14, 9597–9612.

Nanjing Bureau of Ecology and Environment (Njbee), 2017. the communique of Nanjing ecology and environment status (in Chinese). Available at (last access. http://hbj.nanjing.gov.cn/njshjbhj. (Accessed 18 January 2020).

Tao, J., Zhang, L., Cao, J., et al., 2017. A review of current knowledge concerning $PM_{2.5}$ chemical composition, aerosol optical properties and their relationships across China. Atmos. Chem. Phys. 17, 9485–9518.

Wang, H., Qiao, L., Lou, S., et al., 2016. Chemical composition of $PM_{2.5}$ and meteorological impact among three years in urban Shanghai, China. J. Clean. Prod. 112, 1302–1311.

Wu, Y., Zhang, S., Li, M., et al., 2012. The challenge to NO_X emission control for heavy-duty diesel vehicles in China. Atmos. Chem. Phys. 12, 9365–9379.

Xia, Y., Zhao, Y., Nielsen, C., 2016. Benefits of China's efforts in gaseous pollutant control indicated by the bottom-up emissions and satellite observations 2000–2014. Atmos. Environ. 136, 43–53.

Yang, Y., Zhao, Y., 2019. Quantification and evaluation of atmospheric pollutant emissions from open biomass burning with multiple methods: a case study for Yangtze River Delta region, China. Atmos. Chem. Phys. 19, 327–348.

Yang, Y., Liao, H., Lou, S.J., et al., 2014. Decadal trend and interannual variation of outflow of aerosols from East Asia: roles of variations in meteorological parameters and emissions. Atmos. Environ. 100, 141–153.

Yang, Y., Zhao, Y., Zhang, J., et al., 2019. Evaluating the methods and influencing factors of satellite-derived estimates of NO_X emissions at regional scale: a case study for Yangtze River Delta, China. Atmos. Environ. 219, 117051.

Zhang, Q., Zheng, Y., Tong, D., et al., 2019. Drivers of improved $PM_{2.5}$ air quality in China from 2013 to 2017. Proc. Natl. Acad. Sci. Unit. States Am. 116, 24463–24469.

Zhao, Y., Nielsen, C.P., Lei, Y., et al., 2011. Quantifying the uncertainties of a bottom-up emission inventory of anthropogenic atmospheric pollutants in China. Atmos. Chem. Phys. 11, 2295–2308.

Zhao, Y., Qiu, L., Xu, R., et al., 2015. Advantages of city-scale emission inventory for urban air quality research and policy: the case of Nanjing, a typical industrial city in the Yangtze River Delta, China. Atmos. Chem. Phys. 15, 12623–12644.

Zhao, Y., Mao, P., Zhou, Y., et al., 2017a. Improved provincial emission inventory and speciation profiles of anthropogenic non-methane volatile organic compounds: a case study for Jiangsu, China. Atmos. Chem. Phys. 17, 7733–7756.

Zhao, Y., Zhou, Y., Qiu, L., et al., 2017b. Quantifying the uncertainties of China's emission inventory for industrial sources: from national to provincial and city scales. Atmos. Environ. 165, 207–221.

Zhao, Y., Yuan, M., Huang, X., et al., 2020. Quantification and evaluation of atmospheric ammonia emissions with different methods: a case study for the Yangtze River Delta region, China. Atmos. Chem. Phys. 20, 4275–4294.

Zheng, B., Zhang, Q., Tong, D., et al., 2017. Resolution dependence of uncertainties in gridded emission inventories: a case study in Hebei, China. Atmos. Chem. Phys. 17, 921–933.

Zheng, B., Tong, D., Li, M., et al., 2018. Trends in China's anthropogenic emissions since 2010 as the consequence of clean air actions. Atmos. Chem. Phys. 18, 14095–14111.

Zhou, Y., Zhao, Y., Mao, P., et al., 2017. Development of a high-resolution emission inventory and its evaluation and application through air quality modeling for Jiangsu Province, China. Atmos. Chem. Phys. 17, 211–233.